Soils and Foundations 2014;54(4):713–730

HOSTED BY

ELSEVIER

CrossMark

The Japanese Geotechnical Society

Soils and Foundations

www.sciencedirect.com
journal homepage: www.elsevier.com/locate/sandf

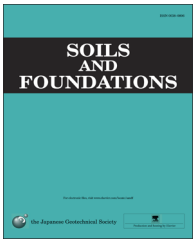

Experimental investigations on suffusion characteristics and its mechanical consequences on saturated cohesionless soil

Lin Ke, Akihiro Takahashi*

Department of Civil Engineering, Tokyo Institute of Technology, Japan

Received 22 August 2013; received in revised form 21 February 2014; accepted 26 March 2014
Available online 20 August 2014

Abstract

The characteristics of suffusion and its mechanical consequences on saturated cohesionless soil with different initial fines contents at various stress states are presented in this paper. A series of seepage tests is performed by constant-flow-rate control mode with the measurement of the induced pore water pressure difference between the top and bottom of the tested specimen under the isotropic confining pressure. Back pressure is maintained constant in the tested soil specimen to ensure fully saturated soil condition. Cumulative eroded soil mass is continuously recorded by a consecutive monitoring system. Suffusion induced axial strain and radial strain of the 70mm-in-diameter and 150mm-in-height specimen is recorded during the seepage tests. The gap-graded cohesionless soil, which are assessed as internally unstable by existing evaluation methods, are tested. The mechanism of suffusion is demonstrated by the variation of hydraulic gradient, hydraulic conductivity, percentage of cumulative fines loss and volumetric strain during suffusion. The parametric study on the influence of two variables, effective stress level and initial fines content, on the mechanism of suffusion is elaborated. The mechanical consequences of suffusion are evaluated by conducting monotonic drained compression tests on the eroded specimens. Companion specimens without suffusion are tested for comparison purpose. The test results reveal that with the progress of suffusion, hydraulic gradient would drop and hydraulic conductivity would increase. Large amounts of fines are eroded away and correspondingly, contractive volumetric strain occurs. The larger effective confining pressure would lead to the less extent of suffusion. With larger initial fines content, more fines would be eroded away. The monotonic compression tests indicate that suffusion would cause the reduction of the soil strength at the major stage of drained shearing.

Keywords: Suffusion; Gap-graded cohesionless soil; Triaxial test; Saturated; Deviator stress

1. Introduction

Significant damage to the high embankments of mountain-side roads was observed during Noto Peninsula Earthquake of Japan in 2007: the road facilities in approximate 80 places have been damaged (Sugita et al., 2008). Significant damage was done to the flow slide of embankments constructed on catchment topography, such as swamps and valleys, which is usually accompanied with a large volume of fresh water. It is possible that those earth structures had suffered from years of erosion, which chronically loosened the soil packing, making it vulnerable to seismic shaking. Indeed, numerous soil structure failures reported in the literature have been attributed to soil erosion. Crosta and di Prisco (1999) presented a slope failure along an old fluvial terrace in Italy. By site investigation and numerical analysis, the authors concluded that seepage erosion, the tunnel scouring in the superficial layers, and the seepage

*Corresponding author.
E-mail addresses: ke.l.aa@m.titech.ac.jp (L. Ke), takihiro@cv.titech.ac.jp (A. Takahashi).
Peer review under responsibility of The Japanese Geotechnical Society.

http://dx.doi.org/10.1016/j.sandf.2014.06.024

Notation

D_x'	Grain size for which x% mass passing is finer of the coarse fraction of a grading curve (mm)
d_x'	Grain size for which x% mass passing is finer of the fines fraction of a grading curve (mm)
D_x	Grain size for which x% mass passing is finer of the filter (mm)
d_x	Grain size for which x% mass passing is finer of the base soil (mm)
e_0	Initial void ratio after saturation
e_c	Void ratio of the suffusional specimen without volumetric deformation
e	Post-suffusion void ratio
ε_v	Suffusion induced volumetric strain (%)
FC	Initial fines content by mass (%)
ΔFC	Cumulative fines loss by mass (%)
k	Hydraulic conductivity (m/s)
p'	Mean effective stress (kPa)
q	Deviatoric stress (kPa)
Q	Inflow rate (m^3/s)
v	Darcy velocity (m/s)
V_f	Volume of fines
V_c	Volume of coarse grains
ΔV_f	Volume of eroded fines
ΔV	Intergranular re-arrangement induced volume change
Λ	Ratio of the increments of void volume to that of solid volume due to particle removal (McDougall and Pyrah, 2004; McDougall et al., 2013)

erosion at the slop toe were the vital factors triggering the failure. Muir Wood (2007) reported that the two large sink-holes formed by internal erosion at the crest of the W.A.C Bennett Dam in Canada presented a significant threat to the dam safety. Richards and Reddy (2007) concluded that approximately half of the world's dam failures have been related to soil erosion. The main triggers for soil erosion are the piping of soil grains through concentrated leaks, backward erosion, suffusion and dispersion. To clearly recognize the seepage-induced internal instability of soil, the clarity of each term by definition is necessary: (1) piping refers to the phenomenon that underground water flows along continuous openings such as cracks, and the soil on the wall of the tubular "pipe" is progressively washed away with the seepage flow, forming several large and instable soil channels which results in a significant loss of soil integrity; (2) backward erosion indicates the erosion of soil grains at the exit of a seepage path, such as the downstream face of a homogeneous embankment, where the erosion resistance of the soil is highly dependent on the hydraulic gradient and the soil stress state; (3) suffusion describes the phenomenon that fine soil grains are eroded through the voids between the coarse grains by seepage flow, usually accompanied by seepage flow over the years; (4) dispersion results from the chemically induced erosion of clay soils which is mostly observed in rainfall erosion. Recent studies revealed that the initiation and progression phases of piping and soil internal erosion may be classified into four mechanisms: (i) suffusion, (ii) contact erosion, (iii) backward erosion, (iv) concentrated leak erosion (Fry, 2012; Fell and Fry, 2013).

This paper focuses on the characteristics of suffusion. At the beginning of the twentieth century, Russian researchers published a comprehensive study about the selective erosion phenomenon of fine grains through a coarse matrix (Goldin and Rumyantsev, 2009). The fine grains are transported through the voids between the larger grains by seepage flow. This phenomenon is referred to as "suffusion" in hydrology or "percolation" in the power industry. It develops chronically with quantities of seepage flow over a period of years. Kovacs (1981) divided suffusion into two subcategories: internal suffusion and external suffusion. "Internal suffusion" occurs when the hydrodynamic forces are large enough to move fine grains from soils, affecting the local hydraulic conductivity. In contrast, the "external suffusion" occurs at the surface of a soil layer, which is "when the volume of the solid matrix is reduced, accompanied by an increase in permeability, but the stability of the skeleton composed of the coarse grains is unaffected". Recently, refinement of the definition is presented. Moffat and Fannin (2006) separated the phenomenon as "suffusion" and "suffosion". They noted that "Internal instability describes the migration of a portion of the finer faction of a soil through its coarser fraction. Redistribution of the finer fraction, termed suffusion, may yield a loss of grain and instigate a process of undermining, termed suffosion." Richards and Reddy (2007) clearly defined suffusion as "the phenomenon that the finer fraction of an internally unstable soil moves within the coarser fraction without any loss of matrix integrity or change in total volume", whereas suffosion, "on the other hand, means the erosion of grains would yields a reduction in total volume and a consequent potential for collapse of the soil matrix". In this paper, the widely accepted term "suffusion" is used.

Soils vulnerable to suffusion are often considered internally unstable, indicating that the constrictions formed by coarser fractions which constitute the soil skeleton are sufficiently large to allow the free passing of fines. A variety of empirical methods have been proposed to assess the instability potential for a soil (U.S. Army Corps of Engineers, 1953; Istomina, 1957 [Ref. Kovacs (1981)]; Kezdi, 1979; Kenney and Lau, 1985, 1986; Burenkova, 1993; Mao, 2005; Chang and Zhang, 2013b; among others). Those investigations introduce the "filter" concept whereby coarser fractions serve as a filter if water flows through. Whether or not the finer fractions would be potentially flushed off depends on the effective grain size ratio between the filter and fines. The ratio should not exceed an empirically derived threshold. The frequently used representative grain sizes are D_{15}', D_{85}' of the coarse fraction, and d_{15}', d_{85}' of the fines fraction in a soil. The effective grain size

ratio virtually represents the slope of a gradation curve which highlights the variation in grain size over a designated interval of the curve. Chapuis (1992) analyzed several empirically derived methods for the internal stability assessment of granular soils and unified the criteria to one parameter which is the slope of the grading curve. Different methods propose different curve slope values. On the other hand, from the perspective of micromechanics, the effective grain size of coarse fractions acclaimed in those methods may represent the constriction size in soil. Terzaghi and Peck (1948) proposed $D_{15}/4$ to quantify the constriction size in filter and then the soil retention criterion $D_{15}/4 < d_{85}$ is derived. Similarly, Kezdi (1979) noted the value of $D_{15}^{'}/4$–$D_{15}^{'}/5$ can approximate the constriction size in the coarse fraction by assuming a contacting spheres packing of soil. Kenney and Lau (1985) inferred the predominant constriction size in the voids of a filter is approximately equal to the grain size of the soil making up the filter for which 25% by weight is finer. Thanks to the advances in computer science, the theoretical assessment of constriction size could be approached in detail. Reboul et al. (2010) and Vincens et al. (2012) summarized the method of evaluating the constriction size distributions of a numerical assembly of spheres which were generated by Discrete Element Method (DEM). The measurement of the void geometry was fulfilled by a radical Delaunay tessellation. Since high computational expense is necessary for such evaluation, a simple probabilistic based alternative is commonly used. Silveira (1965) assessed the soil filtration/retention by analyzing cumulative constriction size distribution (CSD) which was derived from grain size distribution with assumptions of geometric packing. He examined the probability of a soil grain with equivalent size passing through a probable path in a granular medium, which depends on the constriction sizes of the voids and their occurrences within the filter. Locke et al. (2001) and Indraratna et al. (2007) adopted the developed CSD to solve the time-dependent filtration related issues and improve the retention criterion for nonuniform granular filter design, respectively. For a detailed summary of the abovementioned criteria for suffusion assessment, readers are referred to Marot and Benamar (2012).

The initiation of suffusion on potentially unstable soil is triggered if the hydrodynamic forces induced by the seepage flow on soil grains exceed a critical threshold. In laboratory investigations, seepage flow is maintained by assigning a hydraulic pressure difference or a constant water flow. The critical threshold, termed "critical hydraulic gradient" or "critical flow rate", represents the onset of suffusion (Moffat et al., 2011; Richards and Reddy, 2012). Due to the complexity in soil packing, stress state and controlled hydraulic condition, a widely accepted method to determine the critical value may not exist. The adaptability of the recorded data in literature to other regions depends on the similarity of the fluid/soil condition with that in laboratory tests. Here the significance of the stress state is stressed. As is universally recognized, the behavior of soil is highly influenced by its stress state. However, hitherto, the effect of stress state on erosion mechanism is obscure and controversial. Tomlinson and Vaid (2000) concluded that the larger confining pressure may trigger erosion in artificial granular materials at a smaller gradient because of the disturbance of soil arching. This tendency is especially obvious for the soil specimen with small grain size ratio ($D_{15}^{'}/d_{85}^{'}$). Wan and Fell (2004) noted that the degree of compaction had a minor effect on the erosion rate of silty and cohesive natural soils comparing to the water content and corresponding degree of saturation. Bendahmane et al. (2008) showed that for cohesionless soil, the erosion rate tends to increase with the rising of confining pressure. They assumed the existence of a secondary critical gradient. If the assigned hydraulic gradient is below this value, the confining pressure tends to increase the soil resistance to suffusion, whereas the assigned hydraulic gradient is larger than this value, backward erosion begins. Chang and Zhang (2013a) conducted suffusion tests at isotropic stress state, compression stress state and extension stress state. They divided the erosion process into four phases corresponding to the characteristic hydraulic gradient in each. The maximum eroded soil mass was detected at the extension stress state.

For the non-cohesive soils, due to the large amounts of loss in fines, suffusion may render a loose soil structure with increased porosity and hydraulic conductivity. The strength of post-suffusion soil may decrease due to the destructive function of suffusion. Few studies could deliver comprehensive investigations about the consequences of suffusion from the perspective of soil mechanics. Muir Wood et al. (2010) modeled the mechanical consequences of suffusion by two-dimensional discrete element analysis. In their approach, the progress of suffusion was approximated by progressively removing grains from assemblies of circular discs at different stages of shearing. The simulation indicated that suffusion may trigger the soil state changing from "dense" (below the critical state line) to "loose" (above the critical state line). Similarly, Scholtès et al. (2010) noticed that the soil behavior altered from being dilative to contractive when extracting the fine grains. Those zones in the earthen structure where suffusion occurs would be more prone to fail. Xiao and Shwiyhat (2012) conducted undrained compression test on post-suffusion soils and found that the peak deviator stress of suffusional soil was larger than the soil without suffusion, which may be attributed to the low degree of saturation. Hicher (2013) modeled the effects of particle removal on the behavior of granular materials and concluded that removal of soil particles may cause diffuse failure in eroded soil mass.

A comprehensive understanding of the suffusion mechanisms and the post-suffusion soil behavior is beneficial to the estimation of suffusion progress and is helpful for the retrofit of internally eroded soil structures, such as levees. The main purpose of this study is to experimentally investigate the characteristics of suffusion and its mechanical influence on saturated gap-graded cohesionless soil under the isotropic confining pressure using a newly developed triaxial permeameter which is capable of maintaining back pressure in the soil specimen during suffusion test and directly measuring the cumulative eroded soil mass within the test period. The suffusion-induced variation of soil hydraulic conductivity,

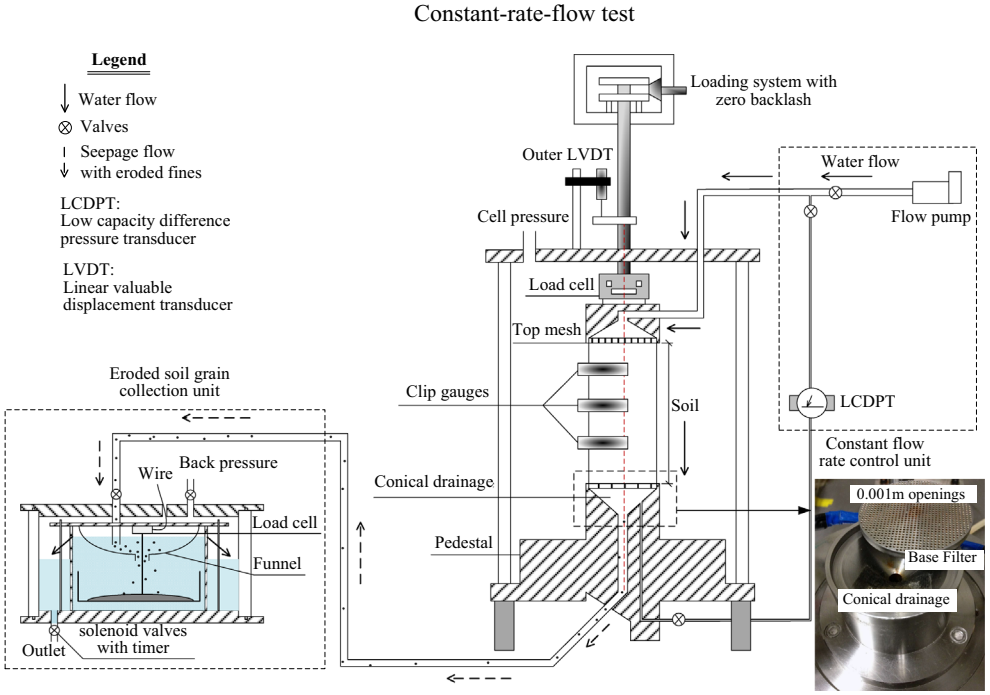

Fig. 1. Schematic diagram of apparatus assembly.

volumetric strain and void ratio is presented. The mechanical consequences of suffusion are revealed by conducting drained monotonic tests on the suffusional specimens and comparing the results with the mechanical responses of companion specimens without suffusion.

2. Experimental investigations

2.1. Triaxial permeameter

The newly developed triaxial cell mainly consists of a constant-flow-rate control unit, an automated triaxial system and eroded soil collection unit. A schematic illustration of the overall system is shown in Fig. 1 (Ke and Takahashi, 2014). The cell accommodates a specimen of 0.07 m-in-diameter and 0.15 m-in-length. The constant-flow-rate control unit is mainly composed of a rotary pump with a maximum flow rate of 2.27×10^{-5} m^3/s for controlling water flow downwardly through the specimen and a Low Capacity Differential Pressure Transducer (LCDPT) for measuring the pressure drop within the tested specimen. The output of LCDPT is highly linear within the range of 0–20 kPa. Two pore pressure transducers are installed at the top and bottom of the specimen respectively to double check the pressure difference. The flow tubes are designated as 0.0075 m-in-diameter. During the experiment, the range of the assigned inflow rate must ensure the resulting pressure drop is well below the confining pressure to prevent the separation of membrane from the specimen. A perforated plate with several 0.001 m openings is mounted in the top cap, to which the specimen is directly attached, to minimize induced head loss. Another plate is at the base pedestal, and serves as a filter (Fig. 1). It is a 0.005 m-thick and 0.07 m-in-dimameter circular steel mesh with a smooth surface. The opening size of the filter is determined as 0.001 m following

Fig. 2. Photography of grains of silica No.3 (left) and No.8 (right).

the specifications of the Japan Dam Conference (Uno, 2009) that the mesh should fully hold the coarse fractions of an unstable soil and allow the passing of fine fractions. A plastic tube is fitted at the outlet of the trough, directly connected to the soil collection system. Downward seepage flow is selected for testing due to the feasibility of triaxial permeameter. It is possible to revise the pedestal to provide sufficient drainage space and conveniently collect eroded fines. Several suffusion tests were conducted by upward seepage flow (Sterpi, 2003). Richards and Reddy (2012) have been reported in the literature, and the conclusion is that the seepage direction significantly altered the critical velocity. A larger value of critical velocity was detected for the tests conducted at the angles between gravitational force and the seepage vector above the horizontal.

The automated triaxial system used could conduct measurements and controls by PC through 16-bit A/D and D/A converters. The vertical load could be automatically applied by a motor-gear system at any rate. The maximum load is

50 kN. The cell pressure is applied by air pressure which is maintained constantly at 700 kPa through an automatic air compressor regulated by E/P (Electronic to Pneumatic) transducers. All the pressure lines are connected to a draining system to remove any condensed water. The deviator load is measured by a submersible load cell mounted inside the cell. The effective pressure is measured by a differential pressure transducer connected between the specimen base and cell. Back pressure is applied from the bottom of the specimen via a 10^{-4} m^3 volume gauge during the consolidation test. Axial displacement is measured externally by a Linear Variable Differential Transformer (LVDT). Three pairs of clip gauges with the maximum capacity of ± 0.002 m are employed to measure the radial strain.

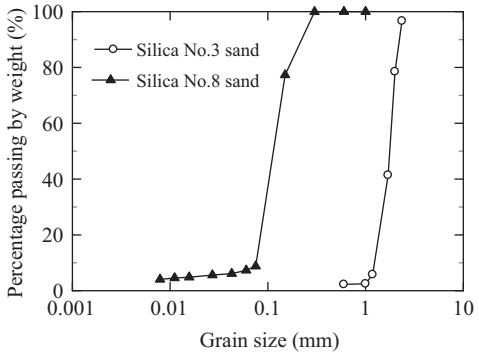

Fig. 3. Grain size distribution curves of silica No.3 and No.8.

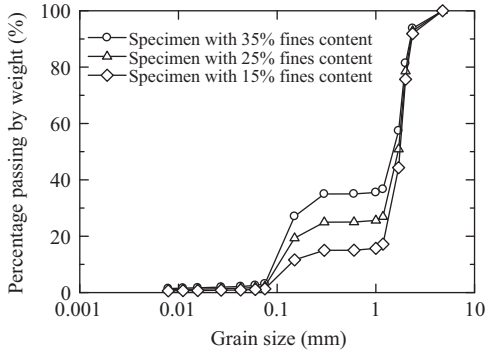

Fig. 4. Grain size distribution curves of the mixtures.

The eroded soil collection unit is the pressured sedimentation tank that consists of the acrylic tube mounted between a steel top and base plate, and sealed by means of O-rings and five external tie rods. A light tray for collecting the eroded soil grains is submerged in a 0.16 m-in-diameter acrylic cylinder and hooked to the load cell, which is attached to a steel frame. A funnel, with a 0.015 m-in-diameter opening at the end is fastened around the inlet pipe to minimize the flow jet effect. The high sensitivity of the waterproof load cell makes it possible to record the mass of eroded soil within the test period. A solenoid valve with a timer is fixed on the outlet drainage line to drain the seepage water away at a determined interval of time. During the suffusion tests, back pressure is applied to the tested specimen from this sedimentation tank.

2.2. Test materials

Gap-graded soils, like sandy gravels, are more prone to suffusion due to their deficiency at certain grain sizes (Skempton and Brogan, 1994). They may be detected at earth dams that have suffered from years of suffusion or at construction sites with substandard procedures of soil mixing, which leads to the omission of amounts of soil grains. In this study, the gap-graded soils consist of the binary mixtures of silica sands (silica No.3 and No.8, shown in Fig. 2) with different dominant grain sizes. The silica sand is mainly composed of quartz, categorized as sub-round to sub-angular material. According to the Unified Soil Classification System

Table 1
Physical properties of tested soil

Physical property	Silica No.3 (coarse fraction)	Silica No.8 (fines)	Specimen 35	Specimen 25	Specimen 15
Specific gravity, G_s	2.645	2.645	2.645	2.645	2.645
Fines content (%)	—	—	35	25	15
Maximum void ratio, e_{max}	0.94	1.33	0.74	0.77	0.79
Minimum void ratio, e_{min}	0.65	0.70	0.36	0.37	0.53
Median particle size D_{50} (mm)[a]	1.76	0.16	1.54	1.68	1.78
Effective particle size D_{10} (mm)	1.77	0.087	0.096	0.109	0.138
Uniformity coefficient C_u	1.5	1.7	18	17	13
Curvature coefficient C_c	1.1	0.96	0.25	7.9	7.9
$(H/F)_{min}$ [b]	—	—	0.05	0.08	0.15
$(D_{15c}/d_{85f})_{gap}$ [c]	—	—	7.9	7.9	7.9
Conditional factor of uniformity, h' [d]	—	—	1.3	1.2	1.2
Conditional factor of uniformity, h'' [e]	—	—	8.5	9.3	6.2
Grain Description	Sub-rounded ~ Sub-angular				

[a] D_X denotes the grain size finer than which the soil weight by percentage is X%.
[b] F is the weight fraction of the soil finer than size d; H is the weight fraction of the soil in the size ranging from d to $4d$.
[c] A soil could be split into the coarse fraction (c) and the fines fraction (f). D_{15c} is the grain size finer than which the soil weight by percentage is 15% for the coarse fraction; d_{85f} is the grain size finer than which the soil weight by percentage is 85% for the fines fraction.
[d] $h'=D_{90}/D_{60}$
[e] $h''=D_{90}/D_{15}$

Table 2
Assessment of the mixture's vulnerability to suffusion.

Criteria	The mixture is internally stable if	Specimen35	Specimen25	Specimen15
U.S. Army (1953)	$C_u < 20$	U[a]	U	S[a]
Istomina (1957) [Ref. Kovacs (1981)]	$C_u \leq 20$	U	U	S
Kezdi (1979)	$(D_{15c}/d_{85f})_{max} \leq 4$	U	U	U
Kenney and Lau (1985, 1986)	$(H/F)_{min} \geq 1$ $(0 < F < 0.2)$	U	U	U
Burenkova (1993)	$0.76log(h'')+1 < h' < 1.86log(h'')+1$	U	U	U
Mao (2005)	$4P_f(1\text{-}n) \geq 1$[b]	U	U	U

[a]"U" means Unstable; "S" means Stable.
[b]P_f is the fines content by weight in soil; n is the porosity, derived from Table 3.

Table 3
Details of test conditions

Specimen	Fines content before suffusion (%)	Initial void ratio	Post consolidation void ratio	Post suffusion void ratio	Mean effective stress (kPa)	Suffusion
35E-50	35	0.64	0.59	1.09	50	Y[a]
35E-100	35	0.60	0.55	0.92	100	Y
35E-200	35	0.59	0.55	0.80	200	Y
25E-50	25	0.61	0.57	0.81	50	Y
15E-50	15	0.68	0.68	0.78	50	Y
35N-50	35	0.60	0.56	—	50	N[b]
25N-50	25	0.61	0.58	—	50	N
15N-50	15	0.68	0.67	—	50	N
35E-50-R	35	0.62	0.60	1.00	50	Y
35E-100-R	35	0.60	0.56	0.95	100	Y
35E-200-R	35	0.64	0.57	0.77	200	Y

[a]"Y" means suffusion;
[b]"N" means no suffusion.

(ASTM D2487-11, 2012), they correspond to SP. The grain size distributions are shown in Fig. 3. In the mixtures, silica No.3 with larger grain size serves as the coarse fraction while the fine silica No.8 is the erodible fines within the voids between the coarse grains. Ke and Takahashi (2012) estimated the maximum mass fraction of fines is approximately 37% for the tested mixtures derived from the geometrical restriction: the volume of fines should be less than that of the voids between coarse grains. A series of fines content (mass ratio of fines to total weight of soil specimen) of 35%, 25% and 15% is adopted. It is worth stressing that maximum mass fraction of fines is derived based on an ideal condition that coarse grains are loosely packed and fines are densely packed between coarse grains. In reality, it is difficult to reach such ideal conditions. Therefore, the maximum mass fraction should be less than 37% depending on the soil fabric and geometry properties of soil grain. The grain size distribution and the physical properties of the mixture are shown in Fig. 4 and Table 1. The vulnerability of the mixture to suffusion is assessed by currently available methods. The details of the evaluation are shown in Table 2, which indicates that the mixtures are potentially unstable for suffusion.

Several internally unstable specimens are tested to understand the suffusion mechanism. A summary of the test cases is shown in Table 3. Each specimen with a moisture content is tamped to the target void ratio. The applied mean effective stress is 50 kPa, 100 kPa and 200 kPa, which approximately corresponds to earth pressures of 5 m, 10 m and 20 m in depth, respectively. In order to understand the mechanical consequences of suffusion, monotonic drained compression is conducted on the suffusional specimens. Controlled specimens (35N-50, 25N-50 and 15N-50) at the same stress state without suffusion are tested for comparison purposes. Three specimens, named 35E-50-R, 35E-100-R and 35E-200-R, are tested at the same effective stress state as that of specimens 35E-50, 35E-100 and 35E-200 to confirm the repeatability of the test results and the apparatus.

3. Test procedures

The moist tamping method (Ladd, 1978) is employed to prepare a specimen for minimizing the segregation of the two different sized grains. The specimen is compacted to the target void ratio by 10 layers and the height of each layer is determined by "undercompaction" at the initial moisture content of 10%. From previous trials and errors, a uniform specimen was achieved at this moisture content. The wet soil is kept in a zipped bag to equalize moisture at least 16 h before use. Since the soil weight could not be directly measured after preparation, the after-test oven-dry weight of the specimen together with the eroded soil weight should be checked. The

reconstituted specimen is 0.07 m in diameter and 0.15 m in height.

The vacuum saturation procedure (JGS 0525-2000, 2000; ASTM D4767-11, 2012) is adopted in this study. Upon the completion of specimen preparation, the top and the bottom of the tested specimen is connected to a lower and an upper reservoir, respectively. Both of the reservoirs are 0.1 m in diameter and 0.3 m in height. Vacuum is supplied to the specimen through both water reservoirs gradually until −80 kPa, keeping the pressure difference inside and outside the specimen constant. Deaerated water in the upper reservoir is slowly injected into the specimen from the bottom. Considering that the tested specimen is internally unstable, the inflow rate should be slow enough to avoid soil grain migration in the specimen (i.e., 5.56×10^{-9} m^3/s). After three-quarters of the deaerated water in the upper reservoir has flowed through the specimen, the vacuum in the specimen is slowly reduced to 0 kPa and the cell pressure is increased to 20 kPa, so that the pressure difference remains constant. Deaerated water is then injected into the specimen again. Deaerated water with a total volume of 10.4 (normalized value in terms of pore volume) flows through the soil specimen before suffusion test. The inlet valve of the sedimentation tank should be closed all the way to avoid any possible soil loss. For the majority of tests, B values of at least 0.95 could be achieved after applying back pressure of 100 kPa following the vacuum saturation procedure.

Consolidation is performed by an automatic control system. Cell pressure gradually increases up to the target value at fairly small increments (i.e., 1 kPa/min) to avoid the migration of soil grains. Axial stress, controlled by a motor, increases correspondingly to keep the determined effective stress ratio (effective axial stress/effective radial stress) constant. In this study, soil specimens are isotropically consolidated until the preferred stress state is reached.

The stress state during the suffusion test is maintained at the same level as that of the isotropic consolidation. The axial displacement, radial deformation, the pore water pressure difference generated by the seepage flow and the cumulative eroded fine mass is recorded at every 1 s automatically. To logically demonstrate the mechanical effects of suffusion on soils, the imposed inflow rate for each specimen is held constant. After several trial tests, an inflow rate of 5.17×10^{-6} m^3/s is selected due to the relatively large fines loss at this rate. The procedure of the inflow rate increments in this study is shown in Fig. 5. The initial increment of inflow rate is set approximately at 1.67×10^{-7} m^3/s per min: the inflow rate is increased to 1.67×10^{-7} m^3/s in 1 min and the seepage is allowed to flow until it becomes steady for the next 1 min. The initiation of suffusion approximately occurs within the inflow rate of 5.00×10^{-7}–1.00×10^{-6} m^3/s. As long as suffusion initiates, the amounts of eroded fine grains increases with the increasing inflow rate. If one wanted to shorten the test, it would be possible to make relatively larger increments at this stage. In this study, the inflow rate is increased to the target value at the incremental rate of 8.33×10^{-7} m^3/s per min. The inflow rate is maintained constant until (1) the recorded hydraulic gradient is steady; (2) the effluence becomes clear and clean by visual observation; (3) no further eroded fines loss occurs (i.e., <0.2 g per 600 s); (4) no further increases in the volumetric strain of the tested specimens is observed. The suffusion tests are terminated at least after 3 h. In most circumstances, the post suffusion B-value is larger than 0.93. During the suffusion test, since the pore pressure at the bottom is maintained constantly at 100 kPa, the downward seepage flow may increase the pore pressure at the top of a tested specimen, and consequently reduce the effective stress linearly along the specimen. The specimen may be unloaded during the suffusion test and a mild recovery of volumetric strain is expected. However, the test results indicate the distribution of effective stress has quite a limited influence on the volumetric strain along the specimen and the hyrdomechanical behavior of tested soil is considered to be mainly governed by the filtration law within the scope of this study. After the suffusion test, a drained compression test is performed at the same stress state as that of the suffusion test to investigate the mechanical consequences of suffusion. The compression test is displacement controlled with an axial strain rate of 0.1%/min, following the standard criteria (JGS 0524-2000, 2000; ASTM D7181-11, 2012), to allow the pore pressure to reach equilibrium. The confining pressure is maintained at a constant while the axial displacement increases at the designated strain rate. Axial stress is obtained from the load cell mounted to the piston. The recorded data from the eroded soil collection unit indicates that there is hardly any fines loss due to compression.

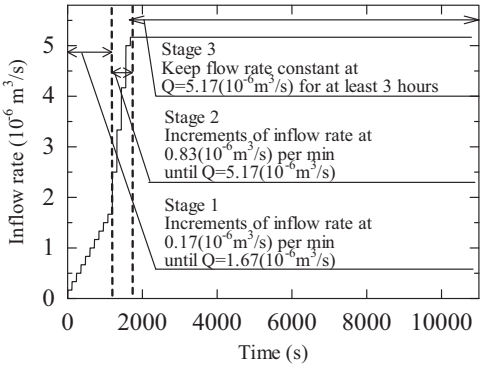

Fig. 5. Inflow rate increments in seepage test.

4. Test results

A parametric study is performed in this series of tests. Two variables in this study are the effective confining pressure (50 kPa, 100 kPa and 200 kPa) and initial fines content (35%, 25% and 15%), which are considered of great significance for the suffusion phenomena. Firstly, the characteristics of suffusion are described by interpreting the hydraulic gradient, cumulative eroded soil mass and volumetric deformation of the tested specimens with 35% initial fines content under the effective confining pressure of 50 kPa (specimen 35E-50). One of the consequences of suffusion is the variation in the grain size distribution curve, which is helpful to illustrate the spatial progression of suffusion. Then, the influence of the two variables is discussed by the comparison of the testing data of other specimens with those of specimen 35E-50.

4.1. Saturation degree

The degree of saturation of the tested specimen tends to decrease during the period of the suffusion test because of the air bubbles generated in the specimen induced by the pore pressure reduction. Commonly, the inflow is at the larger pressure with air dissolved. Due to the head loss during the suffusion test, the pore water pressure in the tested specimens is lower. It is thought that the dissolved air separates out and forms air bubbles in the tested specimen and that the degree of saturation decreases as a result. Evans and Fang (1988) proved that the decrease in the degree of saturation caused a reduction in the measured hydraulic conductivity by approximately three orders of magnitude, which may result in a misleading understanding of the hydraulic behavior of tested sand. Furthermore, a fall in the degree of saturation reduces the quality of the compression test on the suffusional specimens. As a countermeasure, a back pressure of 100 kPa is applied to the tested specimens from the sedimentation tank, shown in Fig. 6. Although slight deviations from 100 kPa exist due to the regular opening/closing of the drainage valve of the sedimentation tank, an attempt is made to maintain the back pressure at a constant in the tested soil specimen. Usually, the *B*-value drops after the suffusion test. For most of the soil specimens, that value is still larger than 0.93, which is considered as fully saturated in this paper.

4.2. Change of hydraulic gradient and conductivity with time

The hydraulic gradient is derived from the recorded pressure drop induced by seepage flow and the specimen length corrected by deducting the vertical deformation. The hydraulic gradient varies corresponding to the progress of suffusion. That variation of specimen 35E-50 at the initial 900 s and 0 s–11,000 s in the suffusion test is plotted in Fig. 7. At 480 s, a moderate drop of hydraulic gradient is noticed (inflow rate $Q=8.33\times10^{-7}$ m^3/s, Darcy velocity $v=2.1\times10^{-4}$ m/s), which is considered as a sign of the onset of suffusion (Fig. 7a). The effluent becomes slightly turbid with very small amounts of suspended fines. At this moment, the reading from the eroded soil collection unit is basically zero, indicating that no eroded fines are detected. It is postulated that at this stage the process of filtration of fine grains diffuses within the specimens. A sharp increase in the hydraulic gradient is detected at 880 s ($Q=1.67\times10^{-6}$ m^3/s, $v=4.2\times10^{-4}$ m/s), at which the increment of the inflow rate begins increasing from 1.67×10^{-7} m^3/s per min to 8.33×10^{-7} m^3/s per min (Fig. 7b). This sharp increase may be related to the influence of "hammer effects" which refers to the phenomenon of sudden increases or decreases in the Darcy velocity which affect the hydraulic properties of soil specimens (Tomlinson and Vaid, 2000), and may induce the unexpected movement of soil grains and cause temporary clogging. The hydraulic gradient dramatically drops after the "peak" with the erosion of a large amount of fines. It is postulated that the soil grains gradually change their position for self-balance at this stage and correspondingly, the specimen deforms. After a certain period, the packing of soil grains reaches a new equilibrium without the further erosion of fines. As a result, the hydraulic gradient becomes constant.

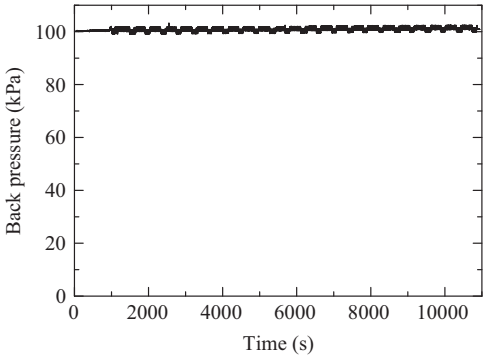

Fig. 6. Maintained back pressure within seepage test period (specimen 35E-50).

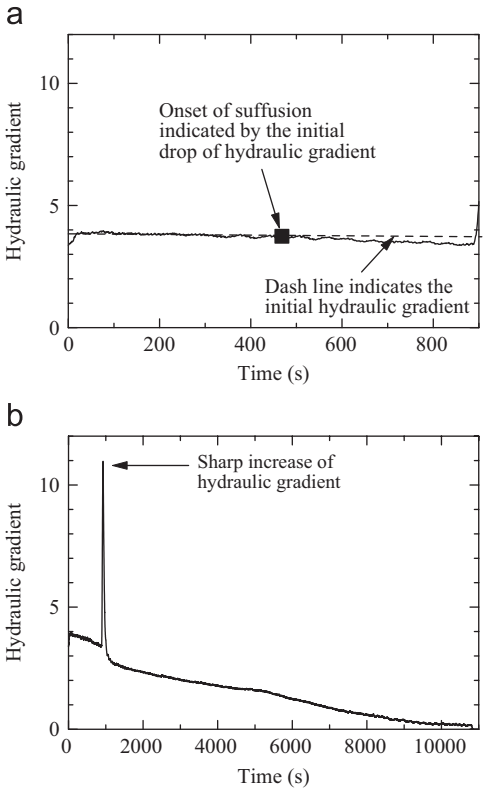

Fig. 7. Hydraulic gradient within seepage test period (specimen 35E-50). (a) 0 s–900 s of seepage test, (b) whole time period of seepage test.

On condition that the Darcy velocity and hydraulic gradient are known, hydraulic conductivity can be calculated following Darcy's law, which describes the flow of a fluid through a porous medium. In this study, inflow is constantly provided by a pump at a constant rate. The discharge rate is unknown due to the difficulties in conducting measurement in a pressurized tank. The Darcy velocity in this assessment is derived from the inflow rate and the cross-sectional area corrected by the radial deformation. Fig. 8 shows the variation of hydraulic conductivity with the period of suffusion test. Before the onset of suffusion, hydraulic

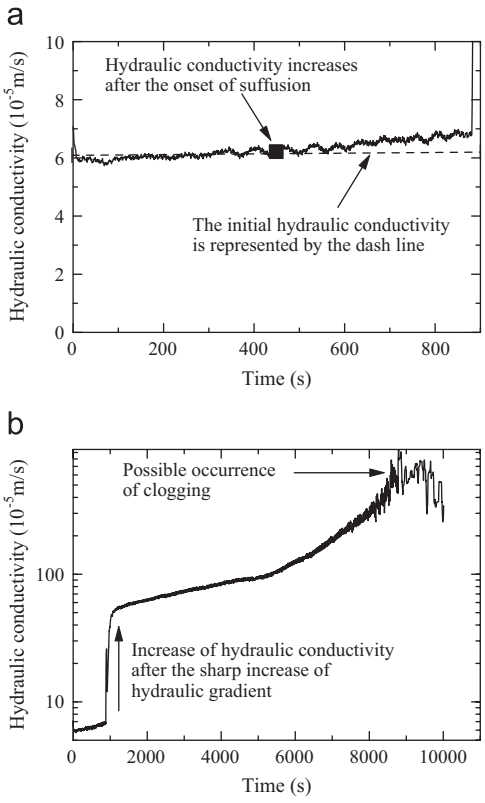

Fig. 8. Hydraulic conductivity within seepage test period (specimen 35E-50). (a) 0 s ~900 s of seepage test, (b) whole time period of seepage test (semi-log scale).

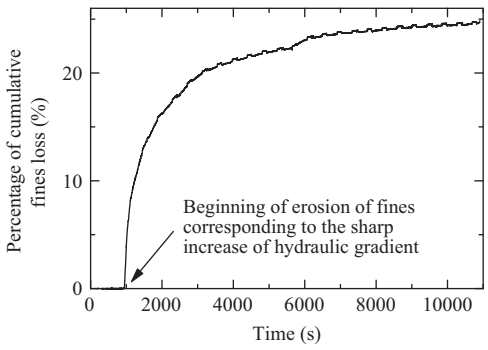

Fig. 9. Percentage of cumulative fines loss within seepage test period (specimen 35E-50).

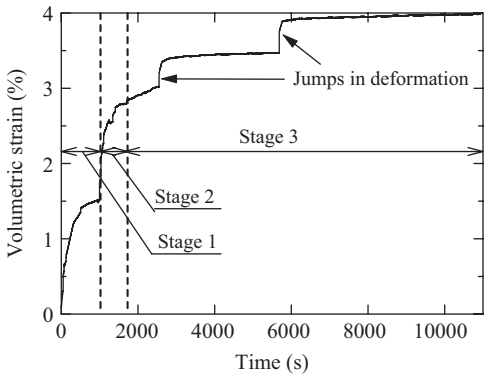

Fig. 10. Volumetric strain within seepage test period (specimen 35E-50).

conductivity is kept constant at 6.0×10^{-5} m/s. At the initial drop of the hydraulic gradient, hydraulic conductivity begins increasing at 480 s ($Q = 8.33 \times 10^{-7}$ m^3/s, $v = 2.1 \times 10^{-4}$ m/s, Fig. 8a). An obvious increase of hydraulic conductivity is observed after the sharp increase of hydraulic gradient (Fig. 8b). It could be understood that with the progress of suffusion, the fines are gradually dislodged, causing an increase in the pore size. Thus, hydraulic conductivity increases. It may be argued that temporary clogging, which leads to the sharp increase of hydraulic gradient, results in a fall in hydraulic conductivity. In this study, the formation and dissipation of the temporary clogging is found to be rapid in a short period probably because of the relatively large hydraulic conductivity of the tested soil. Therefore, a mere increasing of hydraulic conductivity is obviously noted in Fig. 8b. Seepage flow carries a significant amount of fines through the channels formed by voids among coarse grains. It is possible that the movement of fines is impeded at a channel, the size of which is not sufficiently large for the passing of fines and consequently, clogging occurs. With the increasing accumulation of fines at channels, the size of the effective pore throats further decreases and thus, hydraulic conductivity drops. This phenomenon is usually detected after a significant period of time. In this study, the decrease of hydraulic conductivity from 8500 s is most likely an indication of the occurrence of clogging. The maximum hydraulic conductivity detected is approximately 150 times larger than the initial value.

4.3. Cumulative eroded soil mass with time

The evolution of the percentage of cumulative fines loss with time is plotted in Fig. 9 where the recorded cumulative eroded soil mass is normalized by the total weight of specimen before suffusion. Corresponding to the instantaneous increase in the hydraulic gradient, large amounts of fines are eroded away, which might result in an increment of porosity and the re-adjustment of the inter-grain position. The erosion rate decreases with the progress of suffusion. By the end of the test ($t = 11{,}000$ s, $Q = 5.17 \times 10^{-6}$ m^3/s, $v = 1.4 \times 10^{-3}$ m/s), approximately 25% of the fines is lost and 13% remains in the tested specimen.

4.4. Volumetric deformation with time

The incessant erosion of fines from the tested specimen results in the re-arrangement of soil grains, consequently leading to the volumetric deformation. Fig. 10 presents the soil specimen deformation in terms of volumetric strain during the suffusion test. At stage 1 of the suffusion test when the inflow rate increases from 0 until 1.67×10^{-6} m^3/s by 1.67×10^{-7} m^3/s per min, the volumetric strain approximately increases by 2.3% because of the test apparatus. The rotary pump used in the test produces a jet flow on the soil specimen when increasing the inflow rate, i.e., at the beginning of each stage. This jet flow leads to soil deformation, which is considered a limitation of the current water circulation system

of the permeameter. Generally, the tested specimen is prone to be contractive with the progress of suffusion. In stage 3 when the inflow rate is kept constant, two obvious jumps in deformation are detected around 2400 s and 5600 s. It is postulated that along with the constant loss of fines, the coarse grains correspondingly re-arrange their positions to reach a new equilibrium in a short period, which might be an explanation of the sudden and rapid collapse of earthen structures induced by suffusion. Moffat et al. (2011) described the relatively rapid volumetric deformation of soil as one of the characteristics of suffusion.

4.5. Post-suffusion grain size distribution

The variation in grain size distribution reflects the changes in the geometry of soil specimens due to suffusion. Kenney and Lau (1985) concluded that fine grain losses, resulting from suffusion, caused the post-suffusion distribution curve to shift downward from original curve. The extent of the movement proportionally increases with the amount of fine grain loss. Chang and Zhang (2011) experimentally demonstrated that compared to the fines loss in the bottom layer and the middle layer, loss in the upper layer is larger. In this test, the post-suffusion specimen is equally divided into two layers: the top layer and the bottom layer. The grain size distribution curve is determined by the sieving test on those soils that have been oven-dried at 110 °C for 24 h. Fig. 11 presents the typical grain size distributions of a post-suffusion soil specimen. The post-suffusion curves of both the upper layer and bottom layer move downward from the original curve, the extent of which corresponds to the loss of fines. Moreover, the fines loss in the upper layer is more than that in the bottom layer.

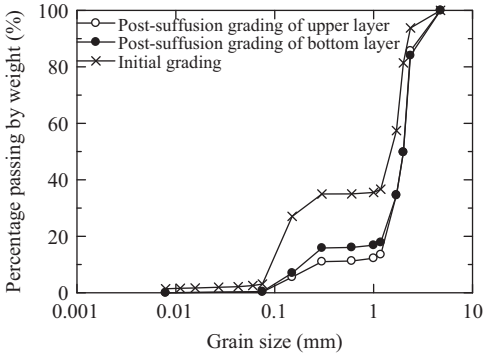

Fig. 11. Grain size distribution curves of the post-suffusion specimen (specimen 35E-50).

Table 4
Assigned Darcy velocity in suffusion tests

Specimen	Darcy velocity (m/s)
35E-50	0.00144
35E-100	0.00150
35E-200	0.00146
25E-50	0.00145
15E-50	0.00138

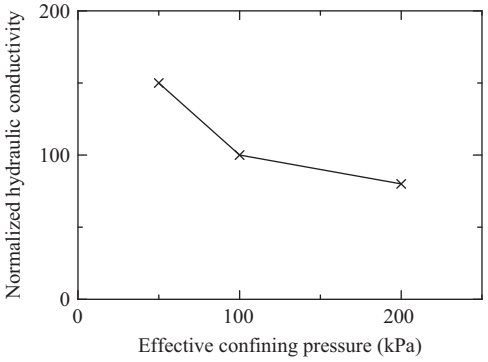

Fig. 12. Normalized hydraulic conductivity versus effective confining pressure for specimens with 35% initial fines content.

4.6. Influence of the effective stress level

Hitherto, it is too complicated to fully understand the effects of the stress level on suffusion. At larger confining pressures, fines are expected to be densely packed among coarse grains and the interstitial spaces are expected to be narrower. For soil specimens with larger confining pressures, seepage flow may well dislodge fewer fines. However, the force transfer mechanism of the granular material is much more complex. Due to the boundary frictions, force-arching may develop at the intersections of the bottom boundary, which may hold the fines from erosion. At larger confining pressures, it is possible that force-arching fails, which, instead, might cause the further erosion of fines. In this study, constant-flow-rate suffusion tests on the specimens with 35% initial fines content under three different effective confining pressures (50 kPa, 100 kPa and 200 kPa) are conducted. Throughout the period of the suffusion test, the mean effective stress is kept the same as that of consolidation (e.g., $p'=50$ kPa, $q=0$ kPa). The influence of effective confining pressure is demonstrated by comparing the test data in terms of Darcy velocity, hydraulic conductivity, percentage of cumulative fines loss and volumetric strain.

The Darcy velocity for stage 3 under different effective confining pressures is presented in Table 4. It indicates that the velocity is basically the same in each case, which provides a reference for the following comparison. Fig. 12 shows the normalized hydraulic conductivity, which is the ratio of the hydraulic conductivity after and before suffusion. For specimen 35E-50, whose effective confining pressure is 50 kPa, the post-suffusion hydraulic conductivity increases nearly 150 times, whereas the increment for specimen 35E-100 and 35E-200 is 100 and 80, respectively. With the progress of suffusion, the specimen gradually becomes heterogeneous and consequently, the local velocity field exhibits significant spatial fluctuations. It is possible that the local flow velocity is different from the overall macroscopic velocity. Under larger effective confining pressures, the maximum value of the local velocity field is lower, and therefore the progress of suffusion may slow down. On the other hand, the fines might be tightly packed and the interlocking between soil grains is firmer under larger effective confining pressure. Thus, fewer fines would overcome the interlocking forces and become dislodged from the specimen, as is shown in Fig. 13.

As is discussed, the extent of the increase in the hydraulic conductivity is closely associated with the amount of fines loss. For specimens with less increase in hydraulic conductivity (i.e., specimen 35E-200), the fines loss is also expected to be less (Fig. 13). Similarly, the volumetric strain induced by erosion of fines is the least in specimen 35E-200 and the largest in specimen 35E-50, shown in Fig. 13.

4.7. Influence of initial fines content

The initial fines content actually characterizes the effect of soil packing, which may offer a physical explanation for the soil hydromechanical behavior. The schematic microstructure of the soil specimen with respective 35%, 25% and 15% fines content is shown in Fig. 14. The majority of the fines is thought to be locked within the voids of coarse grains for the specimen 15E-50 with 15% initial fines content, in contrast with the specimen 35E-50 with 35% initial fines content, where the fines may not only fill the voids but also probably separate the coarse grains. If suffusion initiates, the fines simply occupied the voids may be easily eroded away while those fines separating the coarse grains tend not to move because of the larger contact force on them. Suppose that the fines are merely considered as voids, at the same relative density, the voids size among the coarse grains of specimen 35E-50 would then be larger than that of specimen 15E-50. Thus, a larger void size commonly allows for greater fines loss. Therefore, the specimen with larger initial fines content is assumed to show much greater suffusion.

The Darcy velocity assigned to the specimens with different initial fines contents under an effective confining pressure of 50 kPa is noted in Table 4. A similar value of flow velocity for each specimen is regarded as a reference for comparison. The initial relative density of each specimen is set at 30% for each specimen. The normalized hydraulic conductivity versus initial fines content is presented in Fig. 15, indicating that the largest increase in hydraulic conductivity occurs in specimen 35E-50. Fig. 16 shows the percentage of cumulative fines loss and suffusion-induced volumetric strain versus initial fines content. It can be seen that cumulative fines loss is larger for specimen 35E-50 and correspondingly, the suffusion-induced volumetric strain is larger.

4.8. Test repeatability

Repeatability is confirmed by comparing the key parameters among tested specimens with 35% initial fines content, shown in Table 5. Irregular deviation exists among the hydraulic gradient and hydraulic conductivity, which might be influenced by the inhomogeneity of the specimens. However, the percentage of cumulative fines loss and volumetric strain are basically the same, which might indicate the consistency of erosion law for each test case.

5. Discussions

5.1. Evolution of void ratio

Change of void ratio is caused by the fines loss (ΔV_f) and possible intergranular re-arrangement (ΔV), as is shown in Fig. 17. To address the problem, it is postulated that the void ratio change follows two steps: (1) as soon as suffusion

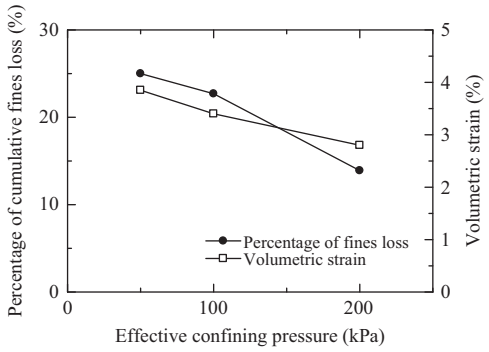

Fig. 13. Percentage of cumulative fines loss and suffusion induced volumetric strain versus effective confining pressure for specimens with 35% initial fines content.

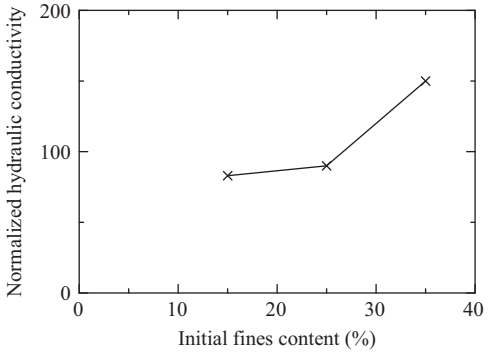

Fig. 15. Normalized hydraulic conductivity versus initial fines content under an effective confining pressure of 50 kPa.

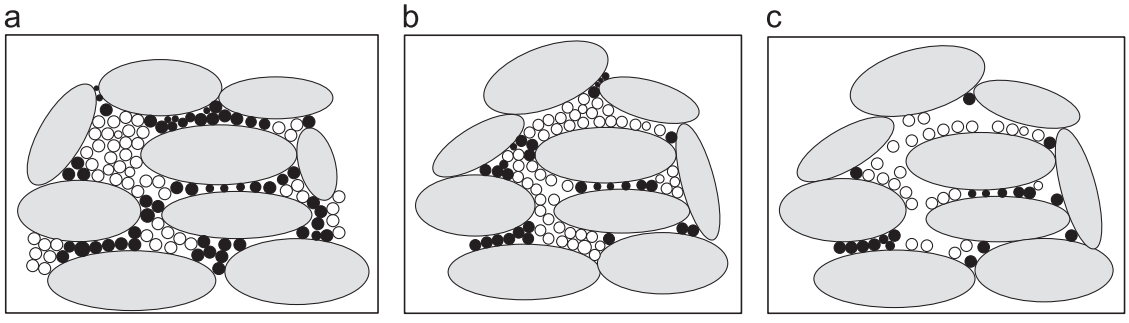

Fig. 14. Schematic diagram of possible soil microstructure (the empty grains are erodible). (a) 35% initial fines content, (b) 25% initial fines content and (c) 15% initial fines content

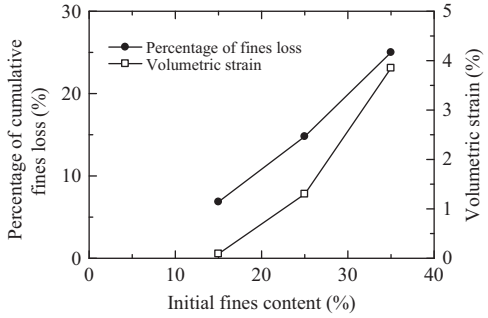

Fig. 16. Percentage of cumulative fines loss and suffusion induced volumetric strain versus initial fines content under an effective confining pressure of 50 kPa.

Table 5
Repeatability of suffusion tests.

Specimen	Maximum hydraulic gradient	Post-suffusion hydraulic conductivity (m/s)	Percentage of cumulative fines loss (%)	Volumetric strain (%)
35E-50	11.7	0.028	25.0	3.9
35E-50-R	10.1	0.019	22.4	3.8
35E-100	5.68	0.008	22.7	3.2
35E-100-R	7.17	0.010	22.7	3.6
35E-200	10.5	0.008	13.9	2.8
35E-200-R	7.76	0.015	16.7	2.8

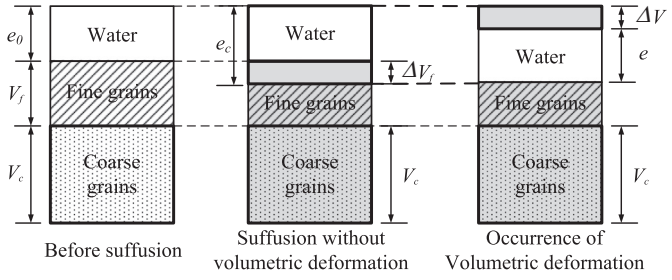

Fig. 17. Suffusion induced variation in soil phase relation.

initiates, no deformation occurs due to the dislodgement of fines, the total volume of the tested specimen remains the same and the volume of eroded fines would be occupied by water at the same volume if the saturated soil is taken into consideration. e_c indicates the void ratio induced by erosion of fines without soil deformation, which can be given by

$$e_c = \frac{e_0 + \Delta FC}{1 - \Delta FC} \tag{1}$$

Where ΔFC indicates the percentage of cumulative fines loss by mass, which is equivalent to the percentage by volume if the specific gravities of the coarse and the fine grains are the same; (2) with the erosion of large amounts of fines, the metastable structure might be formed which easily triggers the re-arrangement of soil grains into a stable packing. Correspondingly, a volumetric deformation (ε_v) and therefore a change in void ratio takes place, which equals to $\varepsilon_v(1+e_c)$. The post-suffusion void ratio is obtained as

$$e = e_c - \varepsilon_v(1+e_c) = (1-\varepsilon_v)\left(\frac{e_0 + \Delta FC}{1 - \Delta FC}\right) - \varepsilon_v \tag{2}$$

As is indicated by Eq. (2), change of void ratio is closely dependent on the volumetric strain during suffusion. If no deformation occurs, a large post-suffusion void ratio is obtained. Further, if the specimen shows dilative behavior during suffusion, the largest void ratio is gained, which may again accelerate the suffusion progress. By contrast, a contraction behavior during this process tends to delay the increase in the void ratio or even result in a decrease in the void ratio after suffusion. Under this circumstance, the lower limit of void ratio can be determined by the greatest density that the coarse grains can achieve. The corresponding volumetric deformation of the specimen reaches the maximum value. Scholtès et al. (2010) conducted simulations of grain extraction using a similar approach. The volumetric deformation (ε_v) of granular assembly was obtained by the analysis of inter-particle sliding resistance. McDougall and Pyrah (2004) and McDougall et al. (2013) proposed a parameter, indicated by Λ, to quantitatively illustrate the dissolution-induced volume change of soil. It is defined as the ratio of the increments of void volume to that of solid volume. A value of -1 indicates no change in volumetric strain and the increase in the void ratio is the maximum.

A plot of the amount of axial, radial and volumetric strain versus cumulative eroded fines loss is depicted in Fig. 18 to interpret the deformation characteristics during suffusion. The positive axial, radial and volumetric strains indicate the contractive behavior of the tested specimen. Initially, the inflow rate is small and few fines are eroded away while the jet flow induced by the flow pump causes certain amounts of strain. From the beginning of stage 2, large amounts of fines are dislodged and soil deformation develops correspondingly. The phenomenon of the jumping of radial strain frequently occurs while the axial strain develops smoothly. Chang and Zhang (2013a) proposed that the soil deformation is mostly determined by the potential of buckling of the strong force chains through the coarse grains and fine grains mainly provide lateral supports for those chains. Since the mass of coarse fractions keeps constant during suffusion, failure of a force chain may let the remaining force chains continue to support the soil specimen and therefore, allow the axial strain to develop smoothly. On the other hand, the fines loss is continuous with the progress of suffusion, which continuously weakens the lateral supports. In certain circumstances, when the remaining fine grains are not strong enough to provide lateral support, sudden radial deformation may occur, which is represented as "jumps" in radial strain. Another potential possibility relates to the strain-measuring techniques employed in the triaxial testing. The axial strain is recorded by an external LVDT, directly connected to the loading piston and top cap. Since the top cap is equally spaced around the top surface of the tested specimen, the measured axial strain actually represents the average displacement, and therefore the recorded curve develops smoothly. For the radial strain determination, on the other hand, it is obtained from three clip gauges attached at the

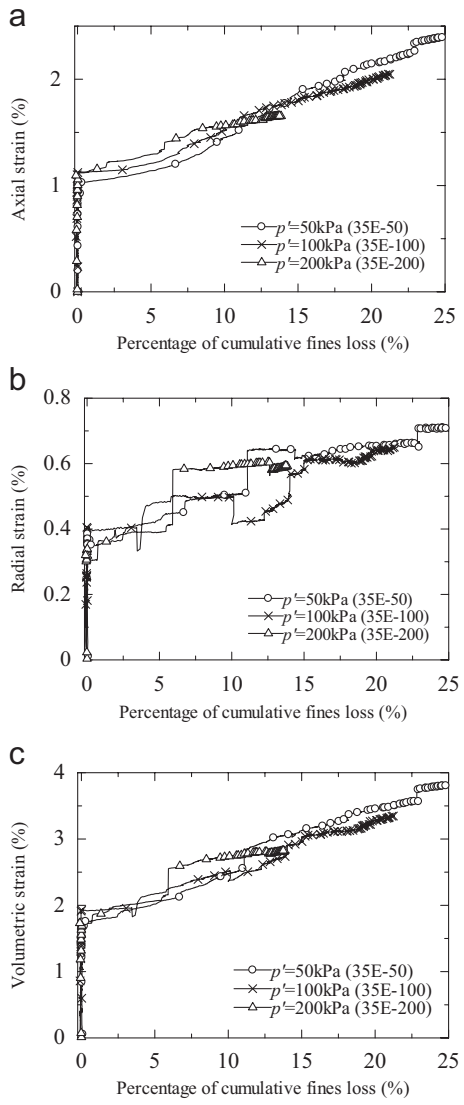

Fig. 18. Axial strain, radial strain and volumetric strain versus percentage of cumulative fines loss under different effective confining pressures for specimens with 35% initial fines content. (a) Axial strain changes, (b) radial strain changes, (c) volumetric strain changes.

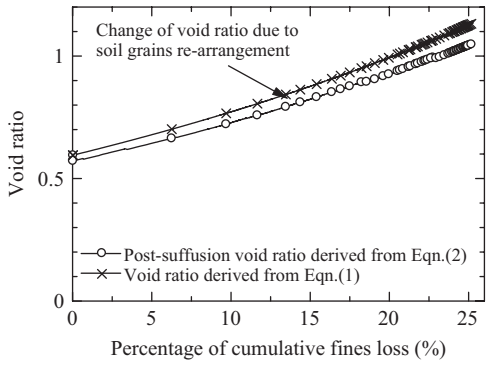

Fig. 19. Void ratio versus percentage of cumulative fines loss under an effective confining pressure of 50 kPa (specimen35E-50).

different spots along the specimen. The inherent assumption is that the average of the discrete radial deformations is representative of the overall radial strain. Compared to the whole body measurements of axial strain, discrete local radial deformation might be discontinuous with possible abrupt irregularities.

The estimated void ratios derived from Eqs. (1) and (2) for the specimens with 35% initial fines content under an effective confining pressure of 50 kPa are presented in Fig. 19, which clearly indicates the contribution of volumetric strain to the void ratio change. For specimen 35E-50, the calculated void ratio considering mere fines loss is 1.13 and because of the volumetric deformation that value approximately decreases by 3.5% to 1.09. The calculated value of Λ is -0.91 for the specimen, indicating a limited influence of volumetric strain on the increments of void ratio. At larger confining pressure, with less loss in fines, the volumetric deformation of the tested specimen and void ratio change is comparatively less. Compared to the soil state before suffusion, the post-suffusion void ratios commonly increase, which might alter the mechanical response of the tested soil in terms of stress–strain relationship.

5.2. Erosion law

The constitutive law for erosion is mostly empirical, derived from laboratory tests. For cohesive soil, Reddi et al. (2000) proposed an expression of shear stress to evaluate the initial surface erosion. Afterwards, a number of internal erosion analysis adopted this concept with the assumption that as long as the seepage flow exerted shear stress is larger than the critical shear stress, erosion occurs (Fujisawa et al., 2010). However, if the size of the flow path within the specimen and that of the eroded fines are considered, there is a high possibility of soil redeposition and clogging. In this paper, the erosion by definition refers to the effective dislodgement and transport of the fines, which is detected at the exit of the tested specimens. The test results are summarized in Figs. 20 and 21 in terms of evolution of (a) percentage of cumulative fines loss with time and (b) erosion rate with hydraulic gradient under different effective confining pressures and initial fines contents. It is noted that both the cumulative eroded soil mass and maximum erosion rate decrease with the effective confining pressure and increase with the initial fines content within the test range. The erosion rate reaches the peak after the onset of suffusion and then drops to a constant value. This tendency is in accordance with the finding made by Reddi et al. (2000), who conducted the laboratory test by a flow pump.

5.3. Mechanical consequences of suffusion

The deviator stress and volumetric strain are plotted versus the axial strain in Figs. 22 and 23 for the respective specimens without and with suffusion. The tested specimens contain 35%, 25% and 15% initial fines content under an effective confining pressure of 50 kPa. The void ratio and fines content before compression are denoted in the figures. By comparing the drained response of the specimens without suffusion, the soil strength and stiffness show a larger value for the less initial fines content, but not much difference can be seen in the volume changes. The exceptional drained response is found in

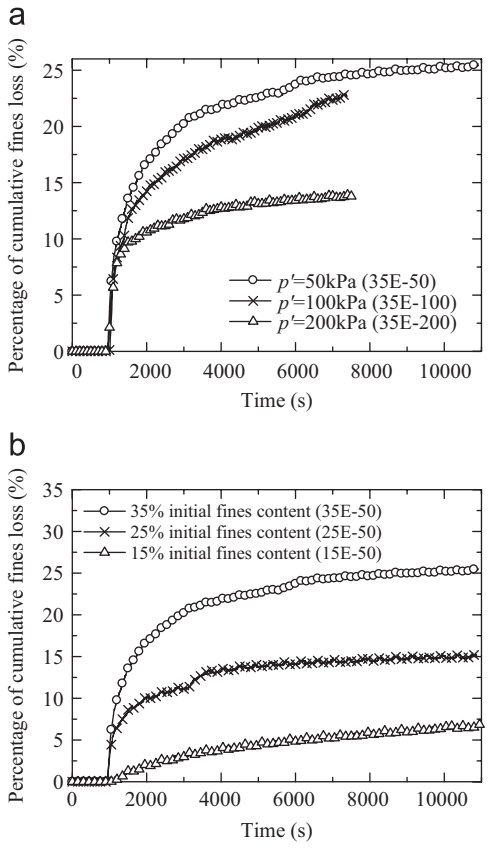

Fig. 20. Percentage of cumulative fines loss within seepage test period.(a) Percentage of cumulative fines loss with time under different effective confining pressures for specimens with 35% initial fines content, (b) percentage of cumulative fines loss with time for specimens with different initial fines contents under an effective confining pressure of 50 kPa.

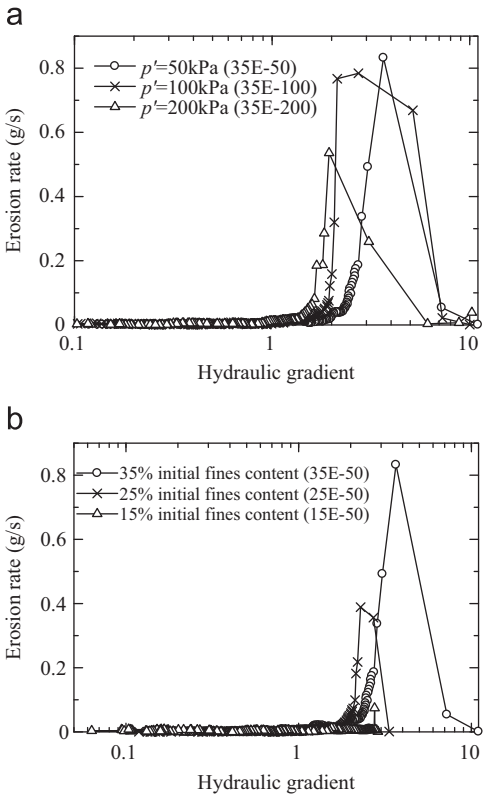

Fig. 21. Evolution of erosion rate with hydraulic gradient (semi-log scale).(a) Erosion rate with hydraulic gradient under different effective confining pressures for specimens with 35% initial fines content, (b) erosion rate with hydraulic gradient for specimens with different initial fines contents under an effective confining pressure of 50 kPa.

specimen 25N-50, which exhibits similar deviator stresses as those of specimen 35N-50 at the medium strain level and relatively large volumetric strain. It may be understood from the characteristics of the soil packing resulting from different fines contents. Previous works noted the fines content was dependent on soil behavior: a threshold fines content, denoting the soil fabric transform between "sand-in-fines" and "fines-in-sand", exists (Vallejo, 2001; Huang et al., 2004; Yang et al., 2006; Shipton and Coop, 2012; among others). The soil with a certain threshold fines content may exhibit a peculiar responses in the deviator stress and volumetric strain compared to those with different fines contents. Chang and Meidani (2013) demonstrated that the fines content of 25% signifies that fines almost occupy the voids of coarse grains and begin separating the sand grains while that larger than 35% stands for the full isolation and floating of coarse grains in a network of fines. Correspondingly, it is inferred that in this study, a fines content of 25% is the threshold value by which specimen 25N-50 appears to behave exceptionally. In terms of the drained response of the specimens with suffusion, since the post-suffusion fines content is quite similar, the behavior is dependent on the void ratio before compression. Specimen 15E-50, which has the least void ratio, shows the largest drained strength and the least ultimate volumetric strain.

The mechanical consequences of suffusion are studied by comparing the drained monotonic compression test results of the suffusional specimens and the companion specimens without suffusion. Muir Wood et al. (2010) concluded that internal erosion (suffusion) lowered the soil strength. Fig. 24–26 plot the stress–strain curves together with the corresponding volumetric strain curves for the compression stage of the soil specimens under an effective confining pressure of 50 kPa. Commonly, the deviator stress of the suffusional specimens is larger at the same small strain level (within 1%) compared to that of the specimen without suffusion while that value becomes less at the same medium level (approximately 1%–16%). In other words, the suffusional soil specimens show a larger initial stiffness at the small strain level, whereas the stiffness of suffusional specimen, conversely, becomes less than the specimen without suffusion when at the medium strain level. For the specimens with the initial fines contents of 25% and 15%, the stress–strain curves of the suffusional soil and the soil without suffusion converge at the large strain level (larger than 16%). The volumetric strain curves appear to be initially contractive then followed by dilation. One exception is found at specimen 35E-50 whereby the specimens of both with and without suffusion show the contractive behavior for the whole shearing stage.

A hypothetical explanation for such inconsistent soil behavior is given at the grain level. In this study, the seepage water

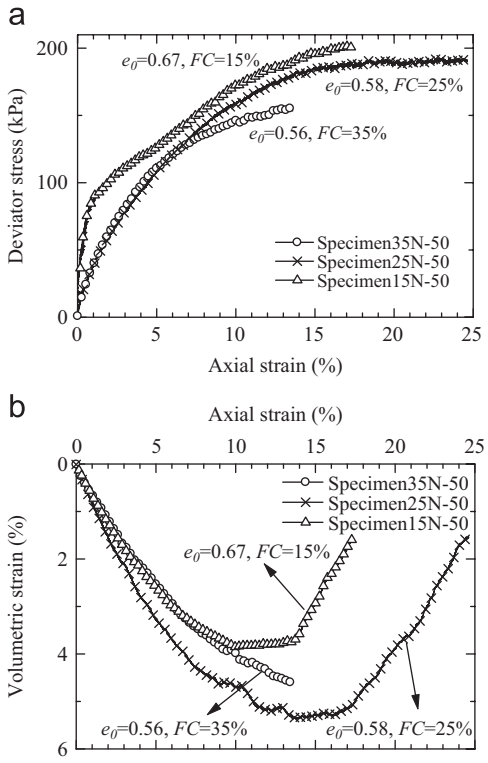

Fig. 22. Summary of drained response of the soil specimens without suffusion (35N-50, 25N-50 and 15N-50) under an effective confining pressure of 50 kPa. (a) Axial strain versus drained deviator stress, (b) axial strain versus volumetric strain.

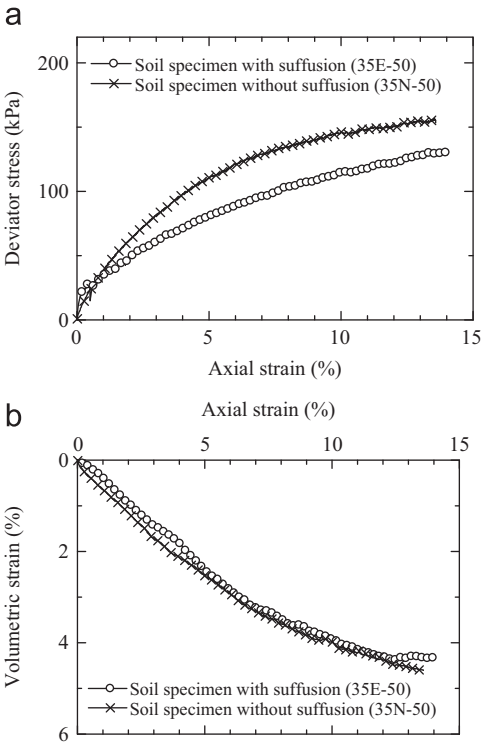

Fig. 24. Comparison of drained response of the soil specimen 35E-50 and 35N-50 under an effective confining pressure of 50 kPa. (a) Axial strain versus drained deviator stress, (b) axial strain versus volumetric strain.

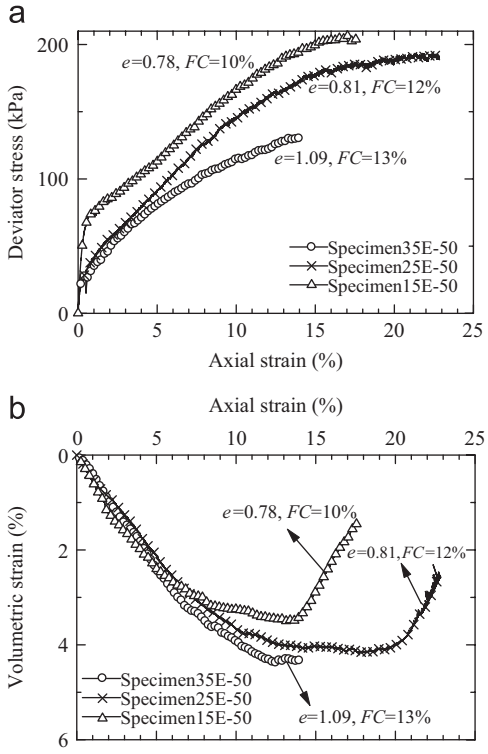

Fig. 23. Summary of drained response of the soil specimens with suffusion (35E-50, 25E-50 and 15E-50) under an effective confining pressure of 50kPa. (a) Axial strain versus drained deviator stress, (b) axial strain versus volumetric strain.

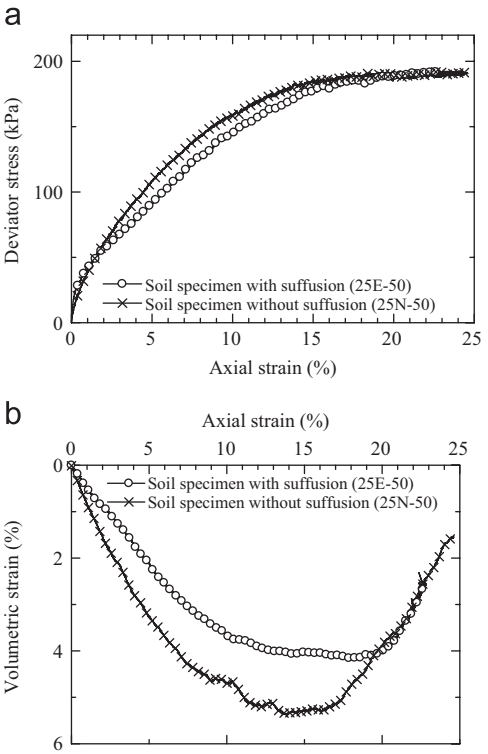

Fig. 25. Comparison of drained response of the soil specimen 25E-50 and 25N-50 under an effective confining pressure of 50 kPa. (a) Axial strain versus drained deviator stress, (b) axial strain versus volumetric strain.

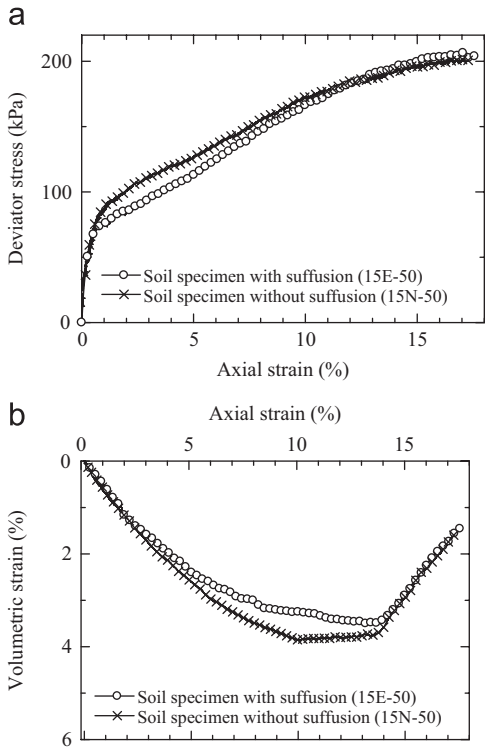

Fig. 26. Comparison of drained response of the soil specimen 15E-50 and 15N-50 under an effective confining pressure of 50 kPa. (a) Axial strain versus drained deviator stress, (b) axial strain versus volumetric strain.

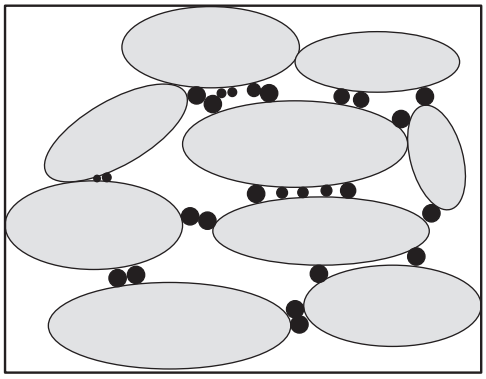

Fig. 27. Possible post-suffusion soil microstructure with fines accumulated at the contact spots among coarse grains.

is fresh water with amounts of fluidized fines. It is possible that the movement of fines is impeded due to the restriction of constriction size and accumulated at the contact points among coarse grains. With the progress of suffusion, the coarse grains are reinforced at those spots where fines have accumulated (Fig. 27). Therefore, the suffusional soil specimens show the larger strength and stiffness at the small strain level (within 1%) with less volumetric deformation. However, the reinforcement may be deteriorated for the subsequent compression, which corresponds to the medium strain level (1%–16%) in this study. To validate this assumption and reveal the mechanical behavior of suffusional soil in detail, microscopic observations of specimens from different levels of shearing may be necessary.

Meanwhile, the influence of the end restraint also needs to be mentioned. The end restraint is a phenomenon in which friction between the tested specimen and the end platens greatly affects the dilation potential of soil at the end zone, causing an unreasonable decrease of pore pressure and increase in the deviator stress. In this study, to ensure the successful drainage of fines, instead of a lubrication layer, a 0.005 m-thick steel mesh with a smooth surface is used, which may have influenced the drained response of the suffusional specimens. It is considered the deemed limitation for compression tests on suffusional soil.

6. Conclusions

The mechanisms of suffusion for saturated sand with different initial fines contents at isotropic stress states are presented in this paper. The binary mixtures consist of two types of silica sands (silica No.3 and No.8) with different dominant grain sizes. With larger grain size, the silica No.3 works as the soil skeleton in the mixtures while the fine silica No.8 is the erodible fines. Suffusion tests are performed by the constant-flow-rate control in triaxial permeameter. The back pressure is applied to ensure the full saturation of tested soil. Cumulative eroded soil mass is continuously recorded by a consecutive monitoring system. The mechanical consequences of suffusion are assessed by conducting drained compression tests on suffusional soil specimens.

Hydraulic gradient dramatically drops with the progress of suffusion, indicated by the erosion of large amounts of fines. Correspondingly, hydraulic conductivity, derived from Darcy's law, keeps increasing at this stage. Afterwards, the soil grains would gradually reach a new equilibrium when the hydraulic gradient and cumulative eroded soil mass become constant. A moderate decrease of hydraulic conductivity is detected after a significantly long period of test time, which might be caused by the clogging of fines inside tested specimens. The erosion of fines results in the increase of contractive volumetric strain. The post-suffusion grain size distribution analysis indicates that the fines loss is larger in the upper layer. The saturation degree drops after suffusion test with the B-value larger than 0.93.

Assigned the seepage flow with the same velocity, the specimens under the larger effective confining pressure show less increments in hydraulic conductivity within the test range. The percentage of cumulative fines loss and volumetric strain induced by suffusion is the least in the specimens under the effective confining pressure of 200 kPa and the largest in the specimens under the effective confining pressure of 50 kPa.

Comparing the suffusion test results of the specimens with 35%, 25% and 15% initial fines content, the largest change in hydraulic conductivity occurs in the specimen with 35% initial fines content. Fines loss is larger for the specimens with larger initial fines content and correspondingly, the suffusion induced volumetric strain is larger. The change of void ratio is closely dependent on the volumetric strain during suffusion. In this series of suffusion tests, the tested specimens show contractive behavior and the post-suffusion void ratio increases.

The deviator stress of the specimens with suffusion is larger at the same small strain level compared to that of the specimens without suffusion. When it comes to the same medium stain level, the specimens with suffusion, however, show less deviator stress. For the specimens with the initial fines contents of 25% and 15%, the stress–strain curves of the suffusional soil and the soil without suffusion converge at the large strain level. In terms of stiffness, the suffusional soil specimens show a larger initial stiffness at the same small strain level, whereas that value becomes less at the same medium strain level. The inconsistency of the eroded soil behavior is assumed to be related to the soil fabric resulting from suffusion. Thus, microscopic observation may be necessary to reveal the mechanism in detail.

Acknowledgment

The first author acknowledges the Japanese Government (Monbukagakusho: MEXT) scholarship support for conducting this research. This work was supported by JSPS KAKENHI Grant nos. 23760440 and 25420498.

References

ASTM D2487-11, 2012. Standard practice for classification of soils for engineering purposes (Unified Soil Classification System). Annual Book of ASTM Standards. ASTM International, West Conshohocken, PA.

ASTM D4767-11, 2012. Standard test method for consolidated undrained triaxial compression test for cohesive soils. Annual Book of ASTM Standards. ASTM International, West Conshohocken, PA.

ASTM D7181-11, 2012. Method for consolidated drained triaxial compression test for soils. Annual Book of ASTM Standards. ASTM International, West Conshohocken, PA.

Bendahmane, F., Marot, D., Alexis, A., 2008. Experimental parametric study of suffusion and backward erosion. J. Geotech. Geoenviron. Eng. 134 (1), 57–67.

Burenkova, V.V., 1993. Assessment of Suffusion in Non-Cohesive and Graded Soils. Filters in Geotechnical and Hydraulic Engineering. Brauns, Heibaum & Schuler, Balkema, Rotterdam, 357–360.

Chang, C.S., Meidani, M., 2013. Dominant grains network and behavior of sand-silt mixtures: stress–strain modeling. Int. J. Numer. Anal. Methods Geomech. 37 (15), 2563–2589.

Chang, D.S., Zhang, L.M., 2011. A stress-controlled erosion apparatus for studying internal erosion in soils. Geotech. Test. J. 34 (6), 579–589.

Chang, D.S., Zhang, L.M., 2013a. Critical hydraulic gradients of internal erosion under complex stress states. J. Geotech. Geoenviron. Eng. 139 (9), 1454–1467.

Chang, D.S., Zhang, L.M., 2013b. Extended internal instability criteria for soils under seepage. Soils Found. 53 (4), 569–583.

Chapuis, R.P., 1992. Similarity of internal stability criteria for granular soils. Can. Geotech. J. 29 (4), 711–713.

Crosta, G., di Prisco, C., 1999. On slope instability induced by seepage erosion. Can. Geotech. J. 36 (6), 1056–1073.

Evans, J.C., Fang, H.Y., 1988, Triaxial permeability and strength testing of contaminated soils. In: Donaghe, R.T., Chaney, R.C., Silver, M.L. (Ed.), Advanced Triaxial Testing of Soils and Rock, ASTM STP 977. American Society for Testing and Materials, Philadelphia, 387-404.

Fell, R., Fry, J.-J., 2013. State of the art on the likelihood of internal erosion of dams and levees by means of testing. In: Bonelli, S. (Ed.), Erosion in Geomechanics Applied to Dams and Levees, Chapter 1. ISTE-Wiley, London, UK, pp. 1–99.

Fry, J.-J., 2012. Introduction to the process of internal erosion in hydraulic structures: embankment dams and dikes. In: Bonelli, S. (Ed.), Erosion of Geomaterials, Chapter 1. ISTE-Wiley, London, UK, pp. 1–36.

Fujisawa, K., Murakami, A., Nishimura, S., 2010. Numerical analysis of the erosion and the transport of fine particles within soils leading to the piping phenomenon. Soils Found. 50 (4), 471–482.

Goldin, A.L., Rumyantsev, O.A., 2009. On the history of development of the seepage and seepage strength of soils issue in Russia and at Vedeneev VNIIG. International Workshop on Internal Erosion in Dams and Foundations, St. Petersburg, Russia, April, 2009.

Hicher, P.-Y., 2013. Modelling the impact of particle removal on granular material behaviour. Géotechnique 63 (2), 118–128.

Huang, Y.T., Huang, A.B., Kuo, Y.C., Tsai, M.D., 2004. A laboratory study on the undrained strength of silty sand from Central Western Taiwan. Soil Dyn. Earthq. Eng. 24, 733–743.

Indraratna, B., Rout, A.K., Khabbaz, H., 2007. Constriction-based retention criterion for granular filter design. J. Geotech. Geoenviron. Eng. 133 (3), 266–276.

Istomina, V.S., 1957. Filtration stability of soils. Gostroizdat, Moscow.

JGS 0524-2000, 2000. Method for Consolidated-Drained Triaxial Compression Test on Soils, Standards of Japanese Geotechnical Society for Laboratory Shear Test. Japanese Geotechnical Society, 23–27.

JGS 0525-2000, 2000. Method for K0 Consolidated-Undrained Triaxial Compression Test on Soils with Pore Water Pressure Measurement, Standards of Japanese Geotechnical Society for Laboratory Shear Test. Japanese Geotechnical Society, 28–34.

Ke, L., Takahashi, A., 2012. Strength reduction of cohesionless soil due to internal erosion induced by one-dimensional upward seepage flow. Soils Found. 52 (4), 698–711.

Ke, L., Takahashi, A., 2014. Triaxial erosion test for evaluation of mechanical consequences of internal erosion. Geotech. Test. J. 37 (2), 347–364.

Kenney, T.C., Lau, D., 1985. Internal stability of granular filters. Can. Geotech. J. 22 (2), 215–225.

Kenney, T.C., Lau, D., 1986. Internal stability of granular filters: reply. Can. Geotech. J. 23 (3), 420–423.

Kezdi, A., 1979. Soil Physics: Selected Topics (Developments in Geotechnical Engineering). Elsevier Science Ltd., Amsterdam, Netherlands.

Kovacs, G., 1981. Seepage Hydraulics. Elsevier Scientific Publishing Company, Amsterdam, Netherlands.

Ladd, R.S., 1978. Preparing test specimens using undercompaction. Geotech. Test. J. 1 (1), 16–23.

Locke, M., Indraratna, B., Adikari, G., 2001. Time-dependent particle transport though granular filters. J. Geotech. Geoenviron. Eng. 127 (6), 521–529.

Mao, C.X., 2005. Study on piping and filters: part 1of piping. Rock Soil Mech. 26 (2), 209–215 (in Chinese).

Marot, D., Benamar, A., 2012. Suffusion, transport and filtration of fine particles in granular soil. In: Bonelli, S. (Ed.), Erosion of Geomaterials, Chapter 2. ISTE-Wiley, London, UK, pp. 39–75.

McDougall, J., Pyrah, I.C., 2004. Phase relations for decomposable soils. Géotechnique 54 (7), 487–493.

McDougall, J., Kelly, D., Barreto, D., 2013. Particle loss and volume change on dissolution: experimental results and analysis of particle size and amount effects. Acta Geotech. 8, 619–627.

Moffat, R.A., Fannin, R.J., 2006. A large permeameter for study of internal stability in cohesionless soils. Geotech. Test. J. 29 (4), 273–279.

Moffat, R., Fannin, R.J., Garner, S.J., 2011. Spatial and temporal progression of internal erosion in cohesionless soil. Can. Geotech. J. 48 (3), 399–412.

Muir Wood, D., 2007. The magic of sands – the 20th Bjerrum Lecture presented in Oslo, 25 November 2005. Can. Geotech. J. 44 (11), 1329–1350.

Muir Wood, D., Maeda, K., Nukudani, E., 2010. Modeling mechanical consequences of erosion. Géotechnique 60 (6), 447–457.

Reboul, N., Vincens, E., Cambou, B., 2010. A computational procedure to assess the distribution of constrictions sizes for an assembly of spheres. Comput. Geotech. 37, 195–206.

Reddi, L.N., Lee, I., Bonala, M.V.S., 2000. Comparison of internal and surface erosion using flow pump tests on a sand-kaolinite mixture. Geotech. Test. J. 23 (1), 116–122.

Richards, K.S., Reddy, K.R., 2007. Critical appraisal of piping phenomena in earth dams. Bull. Eng. Geol. Environ. 66, 381–402.

Richards, K.S., Reddy, K.R., 2012. Experimental investigation of initiation of backward erosion piping in soils. Géotechnique 62 (10), 933–942.

Scholtès, L., Hicher, P.Y., Sibille, L., 2010. Multiscale approaches to describe mechanical responses induced by particle removal in granular materials. C. R. Mec. 338, 627–638.

Shipton, B., Coop, M.R., 2012. On the compression behaviour of reconstituted soils. Soils Found. 52 (4), 668–681.

Silveira, A., 1965. An analysis of the problem of washing through in protective filters. In: Proceedings of 6th International Conference on Soil Mechanics and Foundation Engineering, Montreal, Canada, vol. 2, 551–555.

Skempton, A.W., Brogan, J.M., 1994. Experiments on piping in sandy gravels. Géotechnique 44 (3), 449–460.

Sterpi, D., 2003. Effects of the erosion and transport of fine particles due to seepage flow. Int. J. Geomech. 3 (1), 111–122.

Sugita, H., Sasaki, T., Nakajima, S., 2008. Damage Investigation of Road Embankment Caused by the 2007 Noto Peninsula, Japan Earthquake, Public Works Research Institute Report.

Terzaghi, K., Peck, R.B., 1948. Soil Mechanics in Engineering Practice, 1st edition John Wiley and Sons, New York.

Tomlinson, S.S., Vaid, Y.P., 2000. Seepage forces and confining pressure effects on piping erosion. Can. Geotech. J. 37 (1), 1–13.

Uno, T., 2009. The state of the knowledge on seepage failure phenomena. Geotech. Eng. Mag. 57 (9), 1–5 (in Japanese).

U.S. Army Corps of Engineers, 1953. Filter Experiments and Design Criteria. Technical Memorandum No. 3–360. Waterways Experiment Station, Vicksburg.

Vallejo, L.E., 2001. Interpretation of the limits in shear strength in binary granular mixtures. Can. Geotech. J. 38 (5), 1097–1104.

Vincens, E., Reboul, N., Cambou, B., 2012. The process of filtration in granular materials. In: Bonelli, S. (Ed.), Erosion of Geomaterials, Chapter 3. ISTE-Wiley, London, UK, pp. 81–111.

Wan, C.F., Fell, R., 2004. Investigation of rate of erosion of soils in embankment dams. J. Geotech. Geoenviron. Eng. 130 (4), 373–380.

Xiao, M., Shwiyhat, N., 2012. Experiment investigation of the effects of suffusion on physical and geomechanic characteristics of sandy soils. Geotech. Test. J. 53 (6), 1–11.

Yang, S.L., Sandven, R., Grande, L., 2006. Steady-state lines of sand-silt mixtures. Can. Geotech. J. 43 (11), 1213–1219.